Controlling the Addition of Metal Centers to a Bis(pyrazolyl)methane Starburst Ligand: Direct Routes to Mono-, Bi-, and Trimetallic Rhenium(I) Complexes

Daniel L. Reger,* Russell P. Watson, Mark D. Smith, and Perry J. Pellechia

Department of Chemistry and Biochemistry, University of South Carolina, Columbia, South Carolina 29208

Received October 7, 2005

The bis(pyrazolyl)methane starburst ligand 1,3,5-tris[bis(1-pyrazolyl)methyl]benzene (1,3,5-[CH(pz)$_2$]$_3$C$_6$H$_3$) was prepared by the cobalt-catalyzed condensation reaction between 1,3,5-triformylbenzene and thionyldipyrazole. The addition of Re(CO)$_5$Br to an excess of 1,3,5-[CH(pz)$_2$]$_3$C$_6$H$_3$ resulted in the selective formation of the monometallic complex {1,3,5-[CH(pz)$_2$]C$_6$H$_3$}Re(CO)$_3$Br (**1**). When 2 equiv of Re(CO)$_5$Br was reacted with 1 equiv of 1,3,5-[CH(pz)$_2$]$_3$C$_6$H$_3$, the bimetallic complex {μ-1,3,5-[CH(pz)$_2$]$_3$C$_6$H$_3$}[Re(CO)$_3$Br]$_2$ (**2**) was produced as the major product. The trimetallic complex {μ-1,3,5-[CH(pz)$_2$]$_3$C$_6$H$_3$}[Re(CO)$_3$Br]$_3$ (**3**) was prepared by the reaction of an excess of Re(CO)$_5$Br with 1,3,5-[CH(pz)$_2$]$_3$C$_6$H$_3$. Recrystallization of the complexes from acetone or acetonitrile resulted in the isolation of the crystalline compounds **1**, **1**·(CH$_3$)$_2$CO, **2**·(CH$_3$)$_2$CO, **3**·7CH$_3$CN, **3**·3(CH$_3$)$_2$CO, and **3**·4.5(CH$_3$)$_2$CO. The supramolecular structures of all the complexes are influenced by the 3-fold symmetric, fixed geometry of 1,3,5-[CH(pz)$_2$]$_3$C$_6$H$_3$, and each structure contains intricate networks of molecules, in some cases including alternating layers of complex and solvent molecules, organized through $\pi\cdots\pi$, CH$\cdots\pi$, and other hydrogen-bonding interactions.

Introduction

The coordination chemistry of poly(pyrazolyl)borate and -methane ligands has revealed an impressive number of compounds with interesting structural, catalytic, and electronic properties.[1] The chemistry of poly(pyrazolyl)methane ligands is less extensive than that of their borate analogues due to the fact that convenient syntheses of functionalized neutral methane species have only recently been developed.[2] By functionalizing the pyrazolyl groups in the original poly(pyrazolyl)borate and -methane compounds, a multitude of "second-generation" ligands have been prepared,[1] and more recently, functionalization of the borate or methane backbone has yielded a variety of "third-generation" ligands.[3] Our group has been exploring the coordination chemistry of third-generation bis- and tris(pyrazolyl)methane compounds where two or more of the methane units are linked through organic spacers of varying degrees of flexibility, resulting in multitopic ligands. In addition to the organization imparted by the shape and flexibility of the organic spacer, these ligands are designed to take part in noncovalent interactions that lead to supramolecular structures dominated by $\pi\cdots\pi$ interactions and weak hydrogen bonds, including CH$\cdots\pi$ interactions.[4] Using flexible alkylidene spacers, for example, we investigated the influence of counterion and spacer size on the supramolecular structures of silver(I) complexes in the series of ligands CH(pz)$_2$(CH$_2$)$_n$CH(pz)$_2$ (pz = 1-pyrazolyl; n = 1, 2, 3).[5] Semirigid tris(pyrazolyl)methane ligands, such as C$_6$H$_4$[CH$_2$OCH$_2$C(pz)$_3$]$_2$ (*ortho*, *meta*, and *para*),[6] 1,3,5-(CH$_3$)$_3$C$_6$[CH$_2$OCH$_2$C(pz)$_3$]$_3$,[7] and 1,2,4,5-C$_6$H$_2$[CH$_2$OCH$_2$C(pz)$_3$]$_4$[6a] as well as the ferrocene-linked bis(pyrazolyl)methane

* To whom correspondence should be addressed. E-mail: reger@mail.chem.sc.edu.

(1) (a) Trofimenko, S. *Scorpionates: The Coordination Chemistry of Polypyrazolylborate Ligands*; Imperial College: London, 1999. (b) Trofimenko, S. *Chem. Rev.* **1993**, *93*, 943. (c) Pettinari, C.; Santini, C. *Compr. Coord. Chem. II* **2004**, *1*, 159. (d) Reger, D. L. *Comments Inorg. Chem.* **1999**, *21*, 1. (d) Bigmore, H. R.; Lawrence, S. C.; Mountford, P.; Tredget, C. S. *Dalton Trans.* **2005**, 635. (e) Long, G. J.; Grandjean, F.; Reger, D. L. *Top. Curr. Chem.* **2004**, *233*, 91.

(2) (a) Pettinari, C.; Pettinari, R. *Coord. Chem. Rev.* **2005**, *249*, 525. (b) Pettinari, C.; Pettinari, R. *Coord. Chem. Rev.* **2005**, *249*, 663. (c) Reger, D. L.; Grattan, T. C.; Brown, K. J.; Little, C. A.; Lamba, J. J. S.; Rheingold, A. L.; Sommer, R. D. *J. Organomet. Chem.* **2000**, *607*, 120. (d) Julia, S.; del Mazo, J. M.; Avila, L.; Elguero, J. *Org. Prep. Proc. Int.* **1984**, *16*, 299.

(3) (a) Reger, D. L.; Gardinier, J. R.; Gemmill, W. R.; Smith, M. D.; Shahin, A. M.; Long, G. J.; Rebbouh, L.; Grandjean, F. *J. Am. Chem. Soc.* **2005**, *127*, 2303. (b) Reger, D. L.; Gardinier, J. R.; Bakbak, S.; Semeniuc, R. F.; Bunz, U. H. F.; Smith, M. D. *New J. Chem.* **2005**, *29*, 1035. (c) White, D.; Faller, J. W. *J. Am. Chem. Soc.* **1982**, *104*, 1548. (d) Brock, C. P.; Das, M. K.; Minton, R. P.; Niedenzu, K. *J. Am. Chem. Soc.* **1988**, *110*, 817. (e) Janiak, C.; Braun, L.; Girgsdies, F. *J. Chem. Soc., Dalton Trans.* **1999**, 3133. (f) Kisko, J. L.; Hascall, T.; Kimblin, C.; Parkin, G. *J. Chem. Soc., Dalton Trans.* **1999**, 1929. (g) Hardin, N. C.; Jeffrey, J. C.; McCleverty, J. A.; Rees, L. H.; Ward, M. A. *New J. Chem*. **1998**, *22*, 661. (h) Niedenzu, K.; Trofimenko, S. *Inorg. Chem.* **1985**, *24*, 4222. (i) Jäkle, F.; Polborn, K.; Wagner, M. *Chem. Ber.* **1996**, *129*, 603. (j) Fabrizi de Biani, F.; Jäkle, F.; Spiegler, M.; Wagner, M.; Zanello, P. *Inorg. Chem.* **1997**, *36*, 2103. (k) Herdtweck, E.; Peters, F.; Scherer, W.; Wagner, M. *Polyhedron* **1998**, *17*, 1149. (l) Guo, S. L.; Peters, F.; Fabrizi de Biani, F.; Bats, J. W.; Herdtweck, E.; Zanello, P.; Wagner, M. *Inorg. Chem.* **2001**, *40*, 4928. (m) Guo, S. L.; Bats, J. W.; Bolte, M.; Wagner, M. *J. Chem. Soc., Dalton Trans.* **2001**, 3572. (n) Bieller, S.; Zhang, F.; Bolte, M.; Bats, J. W.; Lerner, H.-W.; Wagner, M. *Organometallics* **2004**, *23*, 2107.

(4) (a) Desiraju, G. R. *Acc. Chem. Res.* **2002**, *35*, 565. (b) Steiner, T. *Angew. Chem., Int. Ed.* **2002**, *41*, 48. (c) Reger, D. L.; Semeniuc, R. F.; Rassolov, V.; Smith, M. D. *Inorg. Chem.* **2004**, *43*, 537, and references therein. (d) Rowland, R. S.; Taylor, R. *J. Phys. Chem.* **1996**, *100*, 7384.

(5) (a) Reger, D. L.; Watson, R. P.; Gardinier, J. R.; Smith, M. D. *Inorg. Chem.* **2004**, *43*, 6609. (b) Reger, D. L.; Gardinier, J. R.; Semeniuc, R. F.; Smith, M. D. *J. Chem. Soc., Dalton Trans.* **2003**, 1712. (c) Reger, D. L.; Gardinier, J. R.; Grattan, T. C.; Smith, M. R.; Smith, M. D. *New J. Chem.* **2003**, *27*, 1670.

(6) (a) Reger, D. L.; Semeniuc, R. F.; Smith, M. D. *J. Organomet. Chem.* **2003**, *666*, 87. (b) Reger, D. L.; Brown, K. J.; Smith, M. D. *J. Organomet. Chem.* **2002**, *658*, 50. (c) Reger, D. L.; Wright, T. D.; Semeniuc, R. F.; Grattan, T. C.; Smith, M. D. *Inorg. Chem.* **2001**, *40*, 6212.

10.1021/om0508684 CCC: $33.50
Publication on Web 12/21/2005

ligand Fe[$C_5H_4CH(pz)_2]_2$,[8] have also been prepared by our group and studied with metal systems that include cadmium,[6c,7] silver,[4,7,8] manganese,[2c,6a] and rhenium.[6b] Finally, we have studied rigid (fixed), phenylene-linked bis(pyrazolyl)methane ligands including the bitopic, tridentate heteroscorpionate *m*-$C_6H_4[C(pz)_2(2\text{-py})]_2$ (py = pyridyl)[9] and the bidentate series *m*- and *p*-$C_6H_4[CH(pz)_2]_2$ and *p*-$C_6H_4[CH(pz^{4Bn})_2]_2$ (pz^{4Bn} = 4-benzyl-1-pyrazolyl).[10]

One goal of our studies is to find efficient routes to heterometallic complexes with homotopic poly(pyrazolyl)-methane ligands. Such complexes offer the potential for unique properties compared with their homometallic analogues.[11] It is often the case that incorporation of metal fragments into multitopic ligands cannot be controlled to the extent that a single species is produced in which free ligating sites are available for coordination to a second metal center in a subsequent reaction.[12] For example, with homobitopic ligands, it is frequently difficult to prepare a monometallic intermediate [Ligand]-[M_1] for use in a subsequent reaction with a different metal system; in many cases, even in reactions that limit the amount of the metal precursor, the bimetallic [Ligand][$M_1]_2$ complex is produced. It is often too tedious or impossible to obtain a practical yield of the desired monometallic complex. For this reason, the construction of heterometallic complexes from homotopic ligands is frequently impractical or unfeasible, and alternative methods are employed.[13]

We have recently reported that by using specific reaction conditions the addition of only one metal center to the rigid homobitopic, phenylene-linked bis(pyrazolyl)methane ligand *m*-$C_6H_4[CH(pz)_2]_2$ is indeed successful.[10] The monometallic complex {*m*-$[CH(pz)_2]_2C_6H_4$}$Re(CO)_3Br$ can be made in good yield, and we have demonstrated its usefulness in producing heterobimetallic complexes by incorporating a platinum(II) center, yielding {μ-*m*-$[CH(pz)_2]_2C_6H_4$}$[Re(CO)_3Br][Pt(p\text{-tolyl})_2]$. This heterometallic complex is the first we have been able to isolate with the symmetrical multitopic ligands we have studied. All previous attempts with other ligands yielded only homometallic complexes.

The successful isolation of {*m*-$[CH(pz)_2]_2C_6H_4$}$Re(CO)_3Br$ prompted us to investigate the series of multimetallic complexes that could potentially be made using a symmetric, tritopic ligand linked by a rigid aromatic group. A similar semirigid tris(pyrazolyl)methane ligand had already been prepared,[7] but based on earlier studies,[9] we reasoned that the utility of a rigid, tritopic tris(pyrazolyl)methane ligand would be limited by low solubility. We report here the preparation of the predictably more soluble bis(pyrazolyl)methane compound 1,3,5-$[CH(pz)_2]_3C_6H_3$ (L), a rigid, tritopic starburst[14] ligand. The topicity and 3-fold symmetry of this ligand provide the potential for a supramolecular chemistry distinct from the rigid bitopic ligands described earlier.[9,10] We have been able to add one, two, and three [$Re(CO)_3Br$] units efficiently and selectively to this new ligand, yielding the following homometallic tricarbonylrhenium(I) compounds: the monometallic {1,3,5-$[CH(pz)_2]_3C_6H_3$}$Re(CO)_3Br$ (**1**), the bimetallic {μ-1,3,5-$[CH(pz)_2]_3C_6H_3$}$[Re(CO)_3Br]_2$ (**2**), and the trimetallic {μ-1,3,5-$[CH(pz)_2]_3C_6H_3$}$[Re(CO)_3Br]_3$ (**3**). The crystalline forms of these complexes include pseudopolymorphic species that show remarkable ordering of solvated molecules and intricate supramolecular structures.

Experimental Section

General Considerations. Air-sensitive materials were handled under a nitrogen atmosphere using standard Schlenk techniques or in a Vacuum Atmospheres HE-493 drybox. All solvents were dried by conventional methods prior to use. The compounds triethyl 1,3,5-benzenetricarboxylate,[15] 1,3,5-tris(hydroxymethyl)benzene,[16] 1,3,5-triformylbenzene,[17] and $Re(CO)_5Br$[18] were prepared following reported procedures. 1,3,5-Triformylbenzene was also prepared as described below using *o*-iodoxybenzoic acid (IBX).[19] All other chemicals were purchased from Aldrich or Fisher Scientific. Pyrazole was purified by sublimation prior to use. Thionyl chloride was distilled prior to use. All other purchased chemicals were used as received. Reported melting points are uncorrected. IR spectra were obtained on a Nicolet 5DXBO FTIR spectrometer. ^1H and ^{13}C NMR spectra were recorded on a Mercury/VX 300 or INOVA 500 spectrometer. All chemical shifts are in ppm and are secondary-referenced using the signals from residual undeuterated solvents. Mass spectrometric measurements were obtained on a MicroMass QTOF spectrometer or on a VG 70S instrument. Elemental analyses were performed on vacuum-dried samples by Robertson Microlit Laboratories (Madison, NJ).

1,3,5-Triformylbenzene. *o*-Iodoxybenzoic acid (7.49 g, 26.7 mmol) was dissolved in 30 mL of dimethyl sulfoxide (DMSO) at room temperature with vigorous stirring over several minutes. To this solution was added a 15 mL DMSO solution of 1,3,5-tris-(hydroxymethyl)benzene (1.00 g, 5.95 mmol). The resulting solution was stirred at room temperature overnight, during which time the solution became cloudy. Saturated aqueous $Na_2S_2O_3$ (30 mL) was added to the system followed by 30 mL of saturated aqueous $NaHCO_3$. The resulting solution was extracted with CH_2Cl_2 (3 × 30 mL), and the combined organic extracts were washed with water (20 mL) and saturated aqueous NaCl (30 mL). After drying over $MgSO_4$, the solvent was removed by rotary evaporation, yielding

(7) Reger, D. L.; Semeniuc, R. F.; Smith, M. D. *Inorg. Chem.* **2003**, *42*, 8137.
(8) Reger, D. L.; Brown, K. J.; Gardinier, J. R.; Smith, M. D. *Organometallics* **2003**, *22*, 4973.
(9) Reger, D. L.; Gardinier, J. R.; Smith, M. D. *Polyhedron* **2004**, *23*, 291.
(10) Reger, D. L.; Watson, R. P.; Smith, M. D.; Pellechia, P. J. *Organometallics* **2005**, *24*, 1544.
(11) (a) Ceccon, A.; Santi, S.; Orian, L.; Bisello, A. *Coord. Chem. Rev.* **2004**, *248*, 683. (b) Fulton, J. R.; Hanna, T. A.; Bergman, R. G. *Organometallics* **2000**, *19*, 602. (c) Fukuoka, A.; Fukagawa, S.; Hirano, M.; Koga, N.; Komiya, S. *Organometallics* **2001**, *20*, 2065. (d) Fabre, S.; Findeis, B.; Trösch, D. J. M.; Gade, L. H.; Scowen, I. J.; McPartlin, M. *Chem. Commun.* **1999**, 577. (e) Schubart, M.; Mitchell, G.; Gade, L. H.; Kottke, T.; Scowen, I. J.; McPartlin, M. *Chem. Commun.* **1999**, 233. (f) Scheider, A.; Gade, L. H.; Breuning, M.; Bringman, G.; Scowen, I. J.; McPartlin, M. *Organometallics* **1998**, *17*, 1642. (g) *Catalysis by Di- and Polynuclear Metal Cluster Complexes*; Adams, R. D., Cotton, F. A., Eds.; Wiley-VCH: New York, 1998, and references therein.
(12) (a) Balzani, V.; Juris, A.; Venturi, M.; Campagna, S.; Serroni, S. *Chem. Rev.* **1996**, *96*, 759. (b) Chong, S. H.-F.; Lam, S. C.-F.; Yam, V. W.-W.; Zhu, N.; Cheung, K.-K.; Fathallah, S.; Costuas, K.; Halet, J.-F. *Organometallics* **2004**, *23*, 4924. (c) Masllorens, J.; Roglans, A.; Moreno-Mañas, M.; Parella, T. *Organometallics* **2004**, *23*, 2533.
(13) For example: (a) Harriman, A.; Hissler, M.; Khatyr, A.; Ziessel, R. *Eur. J. Inorg. Chem.* **2003**, 955. (b) Börje, A.; Köthe, O.; Juris, A. *J. Chem. Soc., Dalton Trans.* **2002**, 843. (c) Lam, S. C.-F.; Yam, V. W.-W.; Wong, K. M.-C.; Cheng, E. C.-C.; Zhu, N. *Organometallics* **2005**, *24*, 4298.
(14) For examples of starburst ligands and their applications, see: (a) Seward, C.; Wang, S. *Comments Inorg. Chem.* **2005**, *26*, 103. (b) Seward, C.; Jia, W.-L.; Wang, R.-Y.; Wang, S. *Inorg. Chem.* **2004**, *43*, 978. (c) Sumby, C. J.; Steel, P. J. *Organometallics* **2003**, *22*, 2358. (d) Wu, Q.; Hook, A.; Wang, S. *Angew. Chem., Int. Ed.* **2000**, *39*, 3933.
(15) Nielsen, A. T.; Christian, S. L.; Moore, D. W.; Gilardi, R. D.; George, C. F. *J. Org. Chem.* **1987**, *52*, 1656.
(16) Cochrane, W. P.; Pauson, P. L.; Stevens, T. S. *J. Chem. Soc. C* **1968**, 630.
(17) Fourmigué, M. Johannsen, I.; Boubekeur, K.; Nelson, C.; Batail, P. *J. Am. Chem. Soc.* **1993**, *115*, 3752.
(18) Schmidt, S. P.; Trogler, W. C.; Basolo, F. *Inorg. Synth.* **1990**, *28*, 160.
(19) (a) Frigerio, M.; Santagostino, M.; Sputore, S. *J. Org. Chem.* **1999**, *64*, 4537. (b) Frigerio, M.; Santagostino, M.; Sputore, S.; Palmisano, G. *J. Org. Chem.* **1995**, *60*, 7272. (c) Nicolaou, K. C.; Mathison, C. J. N.; Montagnon, T. *J. Am. Chem. Soc.* **2004**, *126*, 5192.

0.78 g (81%) of the desired aldehyde. This aldehyde could be used without further purification, but flushing through a plug of silica gel using CH_2Cl_2 as eluent yielded analytically pure product. The aldehyde obtained by this method melted at 154−159 °C (lit.[17] 155−159 °C), and its spectral characterization matched that of previous reports.[16,17]

1,3,5-Tris[bis(1-pyrazolyl)methyl]benzene, 1,3,5-[CH(pz)$_2$]$_3$C$_6$H$_3$ (L). Sodium hydride (1.78 g, 74.2 mmol) was suspended in 250 mL of THF and cooled in an ice−water bath. Pyrazole (5.04 g, 74.0 mmol) was added, and the resulting solution was allowed to stir at 0 °C for 30 min, after which time, thionyl chloride (2.7 mL, 37.0 mmol) was added dropwise. Once the addition was complete, the ice−water bath was removed, and the resulting suspension was allowed to warm to room temperature with stirring over 40 min. 1,3,5-Triformylbenzene (1.00 g, 6.17 mmol) and $CoCl_2$ (0.24 g, 1.85 mmol) were then added at once, and the system was heated at reflux for 20 h. After cooling to room temperature, water (150 mL) was added, and the resulting solution was stirred at room temperature for 1 h. Methylene chloride (100 mL) was added, the layers were separated, and the aqueous phase was extracted with CH_2Cl_2 (2 × 50 mL). The combined organic extracts were washed with water (150 mL) and dried over $MgSO_4$. Removal of the solvent left an off-white solid that was recrystallized from approximately 150 mL of hot absolute ethanol to yield 2.14 g (67%) of a white solid. Mp: 209−210 °C. Anal. Calcd for $C_{27}H_{24}N_{12}$: C, 62.78; H, 4.68; N, 32.54. Found: C, 62.48; H, 4.40; N, 32.32. IR (KBr, cm^{-1}): 3117, 2954, 1516, 1454, 1430, 1388, 1311, 1238, 1197, 1037, 789, 750, 694. ^{1}H NMR (300 MHz, acetone-d_6): δ 7.90 (s, 3 H, C*H*(pz)$_2$), 7.71 (dd, J = 2.4, 0.6 Hz, 6 H, 5-H pz), 7.48 (dd, J = 2.0, 0.6 Hz, 6 H, 3-H pz), 6.78 (s, 3 H, C$_6$*H*$_3$), 6.27 (dd, J = 2.4, 1.8 Hz, 6 H, 4-H pz). ^{13}C NMR (75.5 MHz, acetone-d_6): δ 141.1, 139.3, 130.9, 127.4, 107.2, 77.5. MS ESI(+) *m*/*z* (rel int %) [assgn]: 539 (25) [M + Na]$^+$, 517 (50) [M + H]$^+$, 449 (100) [M − pz]$^+$, 381 (10) [M − pz −Hpz]$^+$.

{1,3,5-[CH(pz)$_2$]$_3$C$_6$H$_3$}Re(CO)$_3$Br (1). A suspension of Re(CO)$_5$Br (0.410 g, 1.01 mmol) in 30 mL of toluene was heated with stirring to ca. 70 °C until the solid was completely dissolved. The hot solution, with the temperature being maintained at 70 °C, was then added by cannula over 8 min to a refluxing 100 mL toluene solution of an excess of 1,3,5-[CH(pz)$_2$]$_3$C$_6$H$_3$ (1.30 g, 2.52 mmol). A white precipitate was soon noticeable. After the addition was complete, the system was stirred at reflux for an additional 5 h and then allowed to cool to room temperature and stir overnight. The white precipitate was isolated by filtration and washed repeatedly with hot toluene until NMR spectroscopy indicated that all the excess ligand had been removed. The yield was 0.45 g (52%). Mp: 260−262 °C (dec). Anal. Calcd for $C_{30}H_{24}BrN_{12}O_3Re$: C, 41.57; H, 2.79; N, 19.39. Found: C, 41.25; H, 2.70; N, 18.87. IR, ν_{CO} (KBr, cm^{-1}): 2027, 1900. ^{1}H NMR (300 MHz, acetone-d_6): δ 8.50 (s, 1 H, C*H*(pz)$_2$[Re]), 8.33 (dd, J = 0.9, 2.7 Hz, 2 H, 5-H pz[Re]), 8.05 (d, J = 2.1 Hz, 2 H, 3-H pz[Re]), 7.84 (s, 2 H, C*H*(pz)$_2$), 7.68 (d, J = 2.4 Hz, 4 H, 5-H pz), 7.48 (d, J = 1.8 Hz, 4 H, 3-H pz), 6.75 (br s, 1 H, 4-H C$_6$H$_3$), 6.63 (t, J = 2.6 Hz, 2 H, 4-pz[Re]), 6.28 (dd, J = 1.7, 2.6 Hz, 4 H, 4-H pz), 5.78 (s, 2 H, 2,6-H C$_6$H$_3$). MS ESI(+) *m*/*z* (rel int %) [assgn]: 889 (15) [M + Na]$^+$, 867 (100) [M + H]$^+$, 787 (30) [M − Br]$^+$, 719 (10) [M − Br − Hpz]$^+$, 517 (5) [M + H − Re(CO)$_3$Br]$^+$, 449 (10) [M − Re(CO)$_3$Br − pz]$^+$. HRMS: Direct probe (*m*/*z*) calcd for $C_{30}H_{24}BrN_{12}O_3Re$, 865.0886; found 865.0886. Crystals suitable for X-ray analysis were grown by the vapor diffusion of Et_2O into 1 mL acetone solutions of the solid.

{μ-1,3,5-[CH(pz)$_2$]$_3$C$_6$H$_3$}[Re(CO)$_3$Br]$_2$ (2). A suspension of Re(CO)$_5$Br (0.79 g, 1.9 mmol) in 50 mL of toluene was heated with stirring to ca. 80 °C until the solid was completely dissolved. The hot solution, with the temperature being maintained at 80 °C, was then added by cannula over 15 min to a refluxing 75 mL toluene solution of 1,3,5-[CH(pz)$_2$]$_3$C$_6$H$_3$ (0.50 g, 0.97 mmol). A white precipitate formed during the addition. After the addition was complete, the system was stirred at reflux for an additional 5 h and then allowed to cool to room temperature and stir overnight. The white precipitate was isolated by filtration, washed with 5 mL of Et_2O, and dried in vacuo to yield 1.05 g of a solid consisting mainly of **2** contaminated with **1** and **3**. Layering Et_2O onto an acetone solution of 0.36 g of the crude product yielded 0.27 g of X-ray quality crystals of analytically pure **2**·(CH$_3$)$_2$CO. X-ray quality crystals could also be grown by the vapor diffusion of Et_2O into acetone solutions of the crude solid. Mp: 290 °C (dec). Anal. Calcd for $C_{36}H_{30}Br_2N_{12}O_7Re_2$: C, 33.92; H, 2.37; N, 13.18. Found: C, 33.87; H, 2.23; N, 13.34. IR, ν_{CO} (KBr, cm^{-1}): 2026, 1899. ^{1}H NMR (300 MHz, acetone-d_6): δ 8.53 (s, 2 H, C*H*(pz)$_2$-[Re]), 8.30 (dd, J = 0.6, 2.7 Hz, 4 H, 5-H pz[Re]), 8.08 (d, J = 2.7 Hz, 4 H, 3-H pz[Re]), 7.81 (s, 1 H, C*H*(pz)$_2$), 7.68 (d, J = 2.4 Hz, 2 H, 5-H pz), 7.49 (d, J = 2.1 Hz, 2 H, 3-H pz), 6.68 (t, J = 2.4, 4 H, 4-pz[Re]), 6.29 (dd, J = 1.7, 2.6 Hz, 2 H, 4-H pz), 5.99 (s, 2 H, 4,6-H C$_6$H$_3$), 5.11 (s, 1 H, 2-H C$_6$H$_3$). MS ESI(+) *m*/*z* (rel int %) [assgn]: 1239 (20) [M + Na]$^+$, 1217 (100) [M + H]$^+$, 1137 (75) [M − Br]$^+$, 867 (35) [M + H − Re(CO)$_3$Br]$^+$, 787 (10) [M − Re(CO)$_3$Br − Br]$^+$. HRMS: Direct probe (*m*/*z*) calcd for $C_{33}H_{24}Br_2N_{12}O_6Re_2$, 1216.9464; found 1216.9423.

{μ-1,3,5-[CH(pz)$_2$]$_3$C$_6$H$_3$}[Re(CO)$_3$Br]$_3$ (3). Re(CO)$_5$Br (0.790 g, 1.95 mmol) and 1,3,5-[CH(pz)$_2$]$_3$C$_6$H$_3$ (0.250 g, 0.484 mmol) were dissolved together in acetone and heated at reflux for 3 days. After removal of the solvent, the crude residue was washed with a 1:1 solution of acetone−hexanes, leaving 0.20 g (26%) of pure **3**. A small amount of impure **3** was also detected in the filtrate, but further purification was not attempted. Mp: 280 °C dec. Anal. Calcd for $C_{36}H_{24}Br_3N_{12}O_9Re_3$: C, 27.59; H, 1.54; N, 10.73. Found: C, 27.69; H, 1.70; N, 10.30. IR, ν_{CO} (KBr, cm^{-1}): 2028, 1883. ^{1}H NMR (300 MHz, acetone-d_6): δ 8.55 (s, 3 H, C*H*(pz)$_2$), 8.26 (d, J = 2.7 Hz, 6 H, 5-H pz), 8.11 (d, J = 2.7 Hz, 6 H, 3-H pz), 6.74 (t, J = 2.4 Hz, 6 H, 4-H pz), 5.83 (s, 3 H, C$_6$*H*$_3$). MS ESI(+) *m*/*z* (rel int %) [assgn]: 1607 (70) [M + K]$^+$, 1487 (100) [M − Br]$^+$. Crystals suitable for X-ray analysis were grown by the vapor diffusion of Et_2O into 1 mL acetone or acetonitrile solutions of the solid.

Crystal Structure Determinations. X-ray intensity data from a colorless bar of **1**·(CH$_3$)$_2$CO, from colorless plates of **1** and **3**·4.5(CH$_3$)$_2$CO, and from colorless prisms of **2**·(CH$_3$)$_2$CO, **3**·7CH$_3$CN, and **3**·3(CH$_3$)$_2$CO were measured at 150(1) K on a Bruker SMART APEX CCD-based diffractometer (Mo Kα radiation, λ = 0.71073 Å).[20] Raw data frame integration and *Lp* corrections were performed with SAINT+.[20] Final unit cell parameters were determined by least-squares refinement of 7707, 8335, 8850, 9965, 8198, and 8621 reflections from the data sets of **1**, **1**·(CH$_3$)$_2$CO, **2**·(CH$_3$)$_2$CO, **3**·7CH$_3$CN, **3**·3(CH$_3$)$_2$CO, and **3**·4.5(CH$_3$)$_2$CO, respectively, each with $I > 5\sigma(I)$. Analysis of the data showed negligible crystal decay during data collection. All data sets were corrected for absorption effects with SADABS.[20] Direct methods structure solution, difference Fourier calculations, and full-matrix least-squares refinement against F^2 were performed with SHELXTL.[21] All non-hydrogen atoms were refined with anisotropic displacement parameters unless otherwise noted. Hydrogen atoms were placed in geometrically idealized positions and included as riding atoms. Details of the data collections are given in Table 1, while further notes regarding the solution and refinement for all six structures follow.

Unsolvated **1** crystallizes in the space group $P2_1/n$ as determined uniquely by the pattern of systematic absences in the intensity data. The asymmetric unit consists of one complete molecule.

The compound **1**·(CH$_3$)$_2$CO crystallizes in the space group $P2_1/n$ as determined uniquely by the pattern of systematic absences in

(20) *SMART* Version 5.625, *SAINT*+ Version 6.22, and *SADABS* Version 2.05; Bruker Analytical X-ray Systems, Inc.: Madison, WI, 2001.

(21) Sheldrick, G. M. *SHELXTL* Version 6.1; Bruker Analytical X-ray Systems, Inc.: Madison, WI, 2000.

Table 1. Crystal Data and Refinement Details for {1,3,5-[CH(pz)$_2$]$_3$C$_6$H$_3$}Re(CO)$_3$Br (1), {1,3,5-[CH(pz)$_2$]$_3$C$_6$H$_3$}Re(CO)$_3$Br·(CH$_3$)$_2$CO (1·(CH$_3$)$_2$CO), {μ-1,3,5-[CH(pz)$_2$]$_3$C$_6$H$_3$}[Re(CO)$_3$Br]$_2$·(CH$_3$)$_2$CO (2·(CH$_3$)$_2$CO), {μ-1,3,5-[CH(pz)$_2$]$_3$C$_6$H$_3$}[Re(CO)$_3$Br]$_3$·7CH$_3$CN (3·7CH$_3$CN), {μ-1,3,5-[CH(pz)$_2$]$_3$C$_6$H$_3$}[Re(CO)$_3$Br]$_3$·3(CH$_3$)$_2$CO (3·3(CH$_3$)$_2$CO), and {μ-1,3,5-[CH(pz)$_2$]$_3$C$_6$H$_3$}[Re(CO)$_3$Br]$_3$·4.5(CH$_3$)$_2$CO (3·4.5(CH$_3$)$_2$CO)

	1	**1**·(CH$_3$)$_2$CO	**2**·(CH$_3$)$_2$CO	**3**·7CH$_3$CN	**3**·3(CH$_3$)$_2$CO	**3**·4.5(CH$_3$)$_2$CO
empirical formula	C$_{30}$H$_{24}$Br-N$_{12}$O$_3$Re	C$_{33}$H$_{30}$BrN$_{12}$-O$_4$Re	C$_{36}$H$_{30}$Br$_2$-N$_{12}$O$_7$Re$_2$	C$_{50}$H$_{45}$Br$_3$N$_{19}$-O$_9$Re$_3$	C$_{45}$H$_{42}$Br$_3$-N$_{12}$O$_{12}$Re$_3$	C$_{49.50}$H$_{51}$Br$_3$-N$_{12}$O$_{13.50}$Re$_3$
fw	866.72	924.80	1274.94	1854.38	1741.24	1828.35
T (K)	150(1)	150(1)	150(1)	150(1)	150(1)	150(1)
cryst syst	monoclinic	monoclinic	triclinic	orthorhombic	monoclinic	triclinic
space group	$P2_1/n$	$P2_1/n$	$P\bar{1}$	$P2_12_12_1$	$P2_1/c$	$P\bar{1}$
a, Å	15.0739(9)	22.5279(12)	8.8952(5)	14.1204(8)	10.6215(5)	13.2164(8)
b, Å	11.7336(7)	12.8446(7)	14.7907(8)	18.5671(11)	14.1987(7)	14.1142(9)
c, Å	18.0498(11)	25.4675(14)	16.1834(9)	24.4197(14)	36.1523(17)	19.1630(12)
α, deg	90	90	89.6620(10)	90	90	95.9450(10)
β, deg	92.7780(10)	103.5980(10)	86.3940(10)	90	92.7560(10)	96.2050(10)
γ, deg	90	90	73.9530(10)	90	90	117.6460(10)
V, Å^3	3188.7(3)	7162.8(7)	2042.0(2)	6402.2(6)	5445.9(5)	3099.6(3)
Z	4	8	2	4	4	2
D(calc), Mg·m^{-3}	1.805	1.715	2.074	1.924	2.124	1.959
abs coeff, mm^{-1}	5.117	4.564	7.943	7.595	8.922	7.844
cryst size, mm^3	0.44 × 0.26 × 0.04	0.40 × 0.20 × 0.16	0.24 × 0.20 × 0.12	0.48 × 0.34 × 0.30	0.26 × 0.20 × 0.12	0.40 × 0.30 × 0.12
final *R* indices [$I > 2\sigma(I)$]						
R1	0.0253	0.0243	0.0410	0.0234	0.0382	0.0389
wR2	0.0625	0.0562	0.0991	0.0551	0.0858	0.0996

Scheme 1

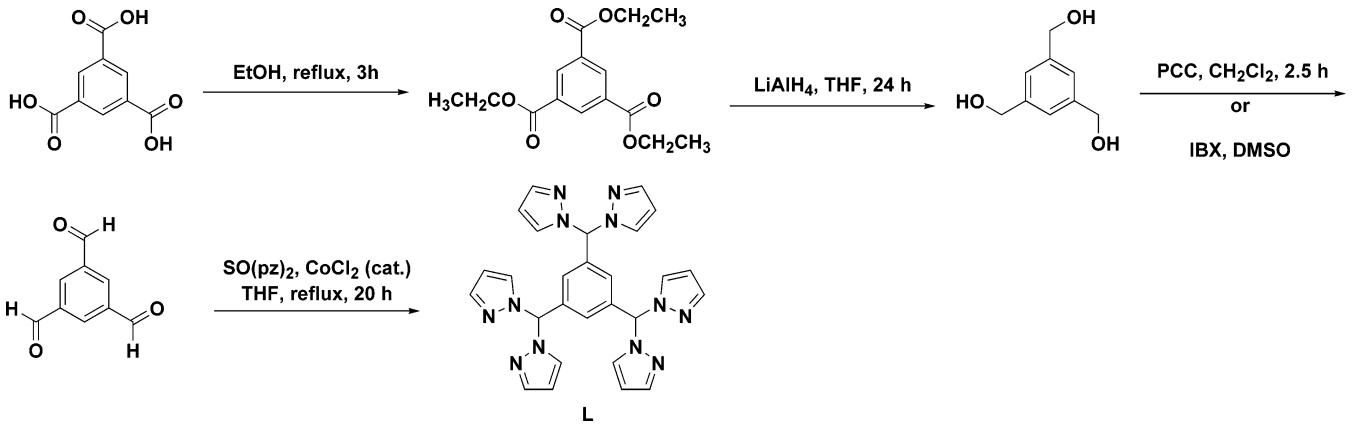

the intensity data. The asymmetric unit consists of two crystallographically independent rhenium complexes and two crystallographically independent acetone molecules of crystallization. Atoms in the rhenium complexes were numbered identically except for the suffix "A" or "B."

The compound **2**·(CH$_3$)$_2$CO crystallizes in the triclinic system. The space group $P\bar{1}$ was assumed and confirmed by the successful solution and refinement of the structure. The asymmetric unit consists of one dirhenium complex and one acetone molecule of crystallization. The acetone molecule was refined using a common isotropic displacement parameter. This molecule likely suffers from minor positional disorder; three distance restraints were used to maintain a reasonable chemical geometry for this species.

The compound **3**·7CH$_3$CN crystallizes in the orthorhombic space group $P2_12_12_1$ as determined uniquely by the pattern of systematic absences in the intensity data. There is one trirhenium complex and seven crystallographically independent, well-ordered CH$_3$CN molecules of crystallization present in the asymmetric unit. The final absolute structure (Flack) parameter refined to −0.011(5), indicating the correct absolute structure and the absence of inversion twinning.

The compound **3**·3(CH$_3$)$_2$CO crystallizes in the space group $P2_1/c$ as determined by the pattern of systematic absences in the intensity data. One Re complex and three independent acetone molecules of crystallization are present in the asymmetric unit. All non-hydrogen atoms were refined with anisotropic displacement parameters except one solvent carbon (C87, isotropic).

The compound **3**·4.5(CH$_3$)$_2$CO crystallizes in the triclinic system. The space group $P\bar{1}$ was confirmed by the successful solution and refinement of the data. There are one Re complex and five independent acetone molecules of crystallization present in the asymmetric unit. One of the acetones (O85) is disordered about an inversion center and was refined as half-occupied. A common isotropic displacement parameter was used for the C and O atoms of this molecule. Acetone O84 was also refined with isotropic displacement parameters. Nine geometric restraints were used to maintain reasonable geometries for these two acetone molecules. All other non-hydrogen atoms were refined with anisotropic displacement parameters.

Results and Discussion

Syntheses and Characterization. The bis(pyrazolyl)methane starburst ligand 1,3,5-[CH(pz)$_2$]$_3$C$_6$H$_3$ (**L**) was prepared in four steps from trimesic acid (1,3,5-benzenetricarboxylic acid), as shown in Scheme 1. Fischer esterification of the acid in absolute ethanol yielded the triethyl ester,[15] which was then reduced to the triol 1,3,5-tris(hydroxymethyl)benzene.[16] At room temperature, this triol was soluble only in water and DMSO, among the common solvents, and its oxidation to 1,3,5-triformylbenzene while co-suspended with pyridinium chlorochromate (PCC) in CH$_2$Cl$_2$[17] proceeded in modest yield. We found, however, that higher yields resulted from using the DMSO-soluble oxidant *o*-iodoxybenzoic acid (IBX).[19] This route was preferred not only

Scheme 2

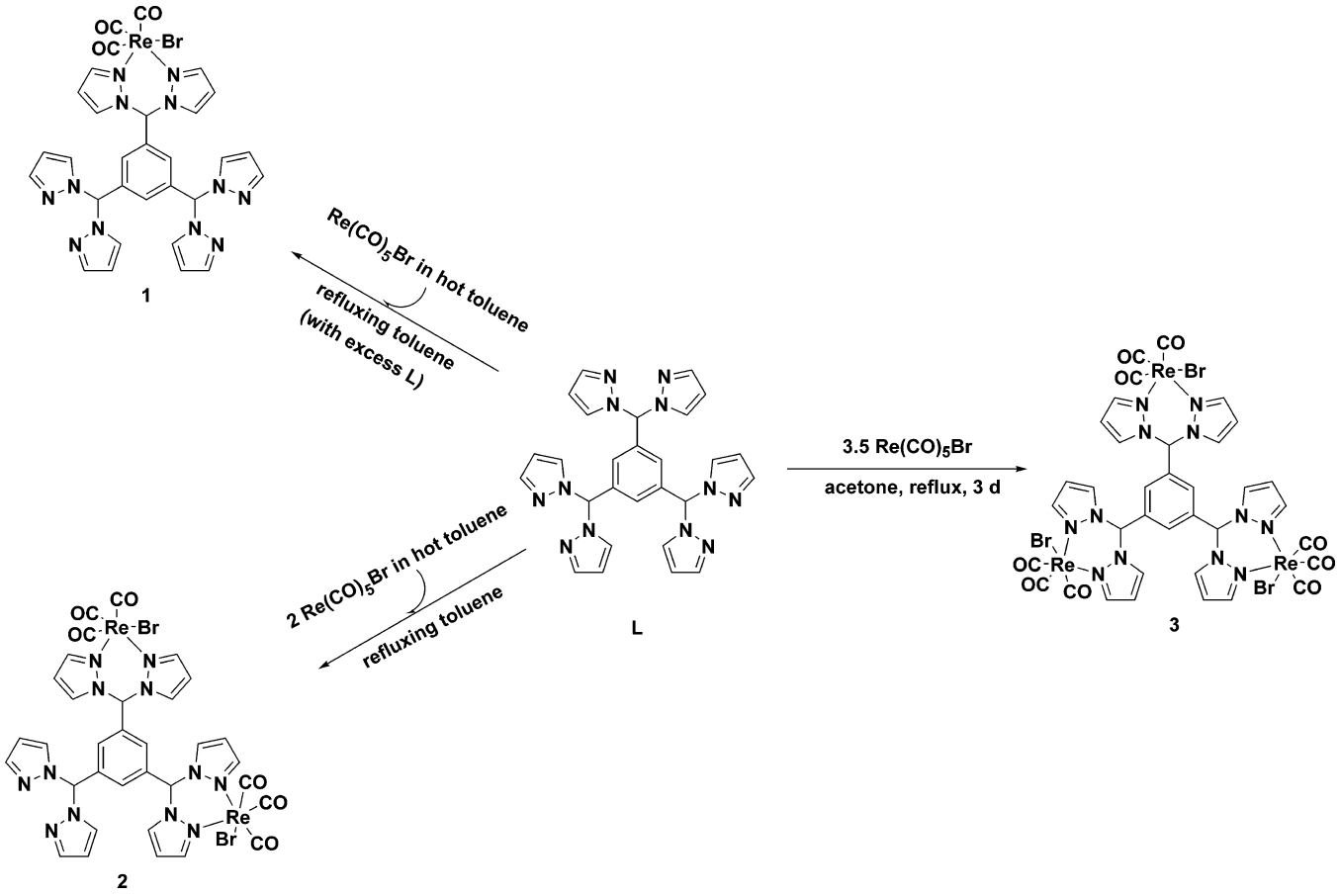

because of the higher yields but also because it included a workup less tedious and hazardous than that for the chromium(VI) reagent PCC (see Experimental Section). Once the aldehyde was obtained, Peterson rearrangement[22] involving the aldehyde and thionyldipyrazole yielded **L** as a white solid freely soluble in halogenated solvents and acetone but with limited solubility in diethyl ether and acetonitrile.

The monometallic complex {1,3,5-$[CH(pz)_2]_3C_6H_3$}$Re(CO)_3Br$ (**1**) was prepared by the dropwise addition of a hot toluene solution of $Re(CO)_5Br$ to a refluxing solution of an excess of **L** (Scheme 2). The precipitated complex could be obtained analytically pure by washing away the leftover **L** with hot toluene. Similarly, the gradual addition of 2 equiv of $Re(CO)_5Br$ in hot toluene to a refluxing toluene solution of 1 equiv of **L** resulted in the formation of the bimetallic complex {μ-1,3,5-$[CH(pz)_2]_3C_6H_3$}$[Re(CO)_3Br]_2$ (**2**) as the major product (Scheme 2) along with the monometallic (**1**) and trimetallic (**3**) complexes as minor products. Judging from ^{1}H NMR spectroscopy, the amounts of **1** and **3** produced as side products varied, but the combined yield of the two impurities could be as high as 33% of the crude product. Recrystallization of this mixture from acetone−Et_2O yielded pure samples of the solvated form **2**·$(CH_3)_2CO$ (see Solid State Structures). The trirhenium complex of **L**, {μ-1,3,5-$[CH(pz)_2]_3C_6H_3$}$[Re(CO)_5Br]_3$ (**3**), was best prepared in acetone according to Scheme 2. Heating an acetone mixture of **L** and a slight excess of $Re(CO)_5Br$ at reflux for 3 days produced **3** in high yield but contaminated with traces of the mono- and dirhenium species. Chromatographic separation of the crude mixture failed, but washing with a minimum amount of a 1:1 acetone−hexanes solution afforded the pure trimetallic complex, albeit in significantly reduced yield due to loss of some of the desired product in the washing step.

Coordination of **L** to $[Re(CO)_3Br]$ can result in stereoisomers that differ in the relative orientation of the methine hydrogen and bromine ligand. NMR and IR spectra, however, indicated that of the two, three, and four possible stereoisomers of the mono-, bi-, and trimetallic complexes, respectively, only one was formed for each complex. The carbonyl stretching frequencies in the infrared indicate local C_{3v} symmetry about rhenium in each complex. The ^{1}H NMR spectra of **1** and **2** are similar in that for each compound there are two sets of bis(pyrazolyl)methane signals reflecting the two distinct chemical environments of the coordinated (bound) and uncoordinated (free) sites. Both complexes possess a plane of symmetry in solution rendering the two free sites of **1** chemically identical and the two bound sites of **2** identical. In **1**, therefore, the ratio of integrations of the free to bound signals is 2:1, and in **2** the same ratio is 1:2. Table 2 compares the chemical shifts of the bis(pyrazolyl)methane units, uncoordinated and coordinated, for the ligand and all three complexes. The respective free sites in both **1** and **2** resonate at approximately the same frequencies as those in the free ligand. The respective coordinated sites in all three complexes also resonate at roughly the same frequencies and are all shifted downfield relative to the free sites.

The three protons on the central arene rings of **1** and **2** are also in two different environments. In **1** there is one proton positioned between two free sites, and it resonates at the same frequency as the arene protons in the free ligand: 6.75 ppm in **1** vs 6.78 ppm in **L**. The other two arene protons in **1** are between both a free site and the coordinated one. These protons

(22) (a) Thé, K. I.; Peterson, L. K. *Can. J. Chem.* **1973**, *51*, 422. (b) Thé, K. I.; Peterson, L. K.; Kiehlman, E. *Can. J. Chem.* **1973**, *51*, 2448. (c) Peterson, L. K.; Kiehlman, E.; Sanger, A. R.; Thé, K. I. *Can. J. Chem.* **1974**, *52*, 2367.

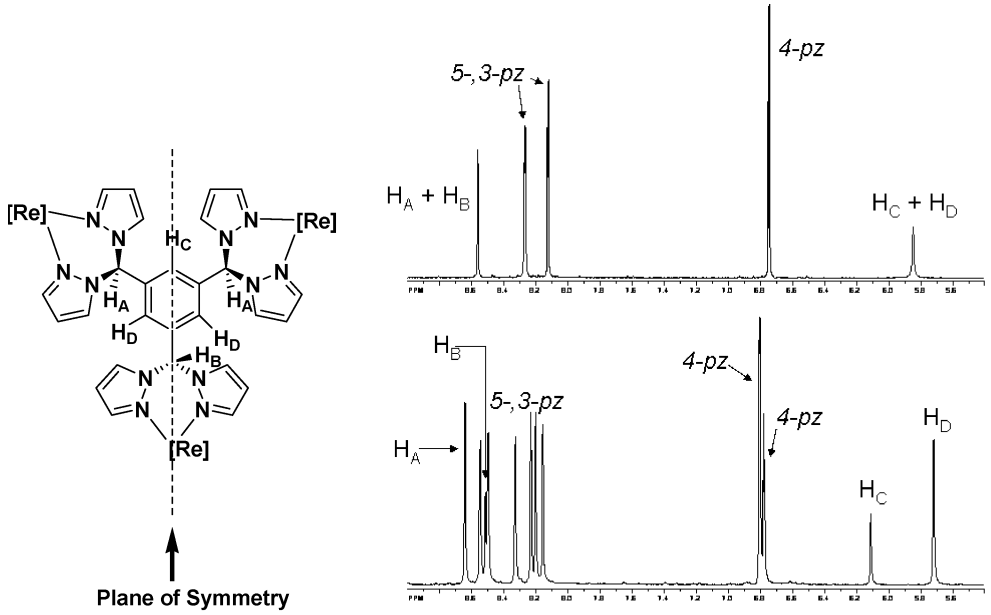

Figure 1. Mirror symmetry of $\{\mu$-1,3,5-$[CH(pz)_2]_3C_6H_3\}[Re(CO)_5Br]_3$ (**3**) in solution (left, [Re] = $[Re(CO)_3Br]$); ^1H NMR spectrum of **3** (500 MHz, acetone-d_6) at 25 °C (top right) and −90 °C (bottom right).

Table 2. Comparison of the Chemical Shifts of Protons Associated with Uncoordinated and Coordinated Ligating Sites in the Ligand (L) and in the Mono- (1), Di- (2), and Trirhenium (3) Complexes of L[a]

Uncoordinated Sites

	methine	5-pz	3-pz	4-pz
L	7.90	7.71	7.48	6.27
1	7.84	7.68	7.48	6.28
2	7.81	7.68	7.49	6.29
3				

Coordinated Sites

	methine	5-pz	3-pz	4-pz
L				
1	8.50	8.33	8.05	6.63
2	8.53	8.30	8.08	6.68
3	8.55	8.26	8.11	6.74

[a] Resonances are in δ units and were recorded at 300 MHz in acetone-d_6 at room temperature.

are shifted upfield of those in the free ligand to 5.78 ppm. In **2** there are also two arene protons between both free and bound sites, and they resonate together at 5.99 ppm. The proton positioned between two bound sites resonates at 5.11 ppm. The three equivalent arene protons in **3**, which resonate at 5.83 ppm, are each between a coordinated site. Unlike the consistent downfield shift of the coordinated pyrazolyl and methine proton signals observed for each complex, there appears to be no trend in the chemical shift of the arene protons that are between a free and a bound site (as in **1** and **2**) or between two bound sites (as in **2** and **3**) other than the fact that the signals of all these protons are shifted upfield of the arene protons in **L**. This upfield shift suggests that the π clouds associated with coordinated pyrazolyl groups provide stronger shielding environments that do the π clouds of uncoordinated pyrazolyl groups. Analyses of the solid-state structures described below support the conclusion that the pyrazolyl rings are responsible for the relative shielding of the arene protons in each complex.

The solution dynamics of the trimetallic complex **3** were further studied using information garnered from its solid-state structure. The geometry observed in crystalline **3** consists of two of the $-CH(pz)_2[Re(CO)_3Br]$ units oriented on one side of the central arene ring with the third on the opposite side (vide infra). The ^1H NMR spectrum of **3** at 25 °C shows a single set of resonances for the complexed ligand that indicates chemical equivalence of all three $-CH(pz)_2[Re(CO)_3Br]$ units as well as of the three protons on the central arene ring (Figure 1). At −90 °C, however, the spectrum shows the complexity expected of **3** if it were to adopt a "two up−one down" conformation as observed in its crystal structure. The rapid equilibration on the NMR time scale that occurs at 25 °C begins to slow appreciably near −10 °C, as indicated by a noticeable broadening of the signals. Using line shape analysis to determine the rate of exchange at varying temperatures, an Arrhenius plot was generated (see Supporting Information), from which the free energy of rotation of the $-CH(pz)_2[Re(CO_3Br]$ groups about the central arene ring was calculated to be 31 kJ/mol.

Solid-State Structures. When $\{1,3,5$-$[CH(pz)_2]_3C_6H_3\}Re(CO)_3Br$ (**1**) is recrystallized from acetone−diethyl ether, two pseudopolymorphic species are isolated from the same mother liquor. The more abundant crystals are colorless plates of the unsolvated complex **1**. Less abundant are colorless needles of the solvated complex $\{1,3,5$-$[CH(pz)_2]_3C_6H_3\}Re(CO)_3Br\cdot(CH_3)_2CO$ (**1**·$(CH_3)_2CO$). Both species crystallize in the monoclinic space group $P2_1/n$. Figure 2 shows ORTEP representations of the metal complexes in each form. The solvated species contains two crystallographically independent complex molecules, labeled here as **1a**·$(CH_3)_2CO$ and **1b**·$(CH_3)_2CO$. Selected bond distances and angles for each species are given in Table 3. The most salient difference between the two crystalline species is the positions of the pyrazolyl rings of the free bis(pyrazolyl)methane units in reference to the plane defined by the central arene ring. In both forms the coordinated bis(pyrazolyl)methane unit lies almost entirely on one side of the ring. In the nonsolvated crystal, for each of the free bis(pyrazolyl)methane units one of the pyrazolyl rings is on one side of the arene plane and the other is on the opposite side (Figure 3, top). The solvated form, however, adopts a conformation in which *all four* of the pyrazolyl rings of the free bis(pyrazolyl)methane units are completely or almost completely on the same side of the central ring as the coordinated bis(pyrazolyl)methane unit (Figure 3, bottom). This conformation is not observed in any of the bi- or trimetallic species discussed below and has only been observed

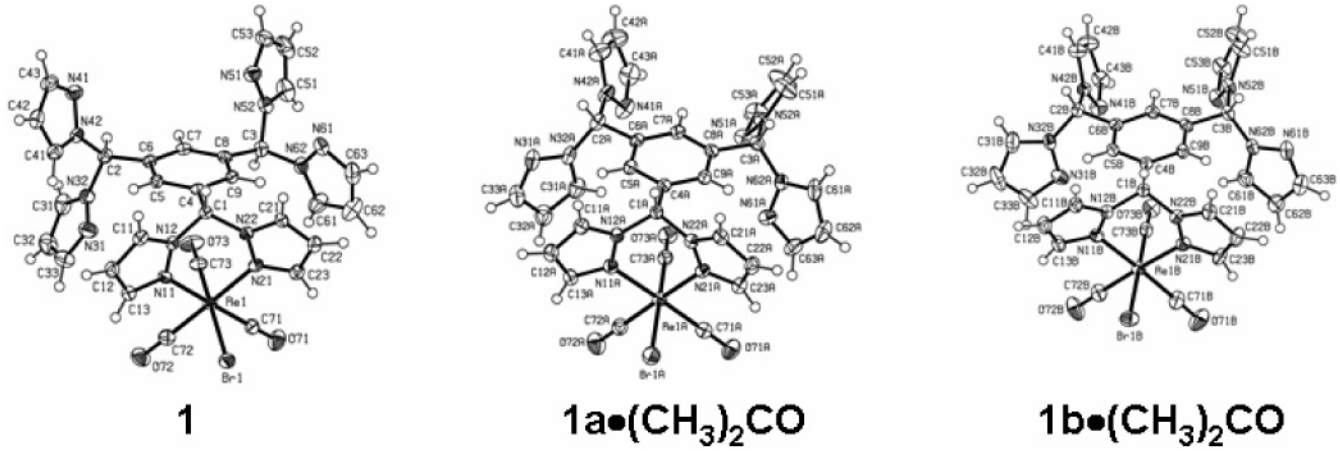

Figure 2. ORTEP drawings of the monometallic molecules of {1,3,5-[CH(pz)$_2$]$_3$C$_6$H$_3$}Re(CO)$_3$Br (**1**) and {1,3,5-[CH(pz)$_2$]$_3$C$_6$H$_3$}Re(CO)$_3$Br·(CH$_3$)$_2$CO (**1**·(CH$_3$)$_2$CO). The two crystallographically independent molecules of **1**·(CH$_3$)$_2$CO are labeled **1a**·(CH$_3$)$_2$CO and **1b**·(CH$_3$)$_2$CO. Ellipsoids are drawn at the 50% probability level.

Table 3. Selected Bond Distances (Å) and Angles (deg) for 1 and 1·(CH$_3$)$_2$CO[a]

	1	**1a**·(CH$_3$)$_2$CO	**1b**·(CH$_3$)$_2$CO
Re(1)−N(11)	2.175(3)	2.181(2)	2.181(2)
Re(1)−N(21)	2.178(2)	2.176(2)	2.173(2)
Re(1)−C(71)	1.915(4)	1.907(3)	1.905(3)
Re(1)−C(72)	1.914(3)	1.909(3)	1.914(3)
Re(1)−C(73)	1.901(3)	1.909(3)	1.915(3)
Re(1)−Br(1)	2.6440(3)	2.6271(3)	2.6183(3)
N(11)−Re(1)−N(21)	83.96(9)	84.72(8)	85.86(8)
N(11)−Re(1)−Br(1)	86.54(6)	83.49(6)	81.27(6)
N(21)−Re(1)−Br(1)	83.93(7)	82.86(6)	83.64(6)
C(71)−Re(1)−Br(1)	90.60(9)	91.36(8)	92.85(10)
C(71)−Re(1)−N(11)	176.26(10)	174.27(10)	175.10(11)
C(71)−Re(1)−C(72)	91.17(13)	89.67(12)	88.58(13)

[a] The two crystallographically independent molecules of **1**·(CH$_3$)$_2$CO are denoted as **1a**·(CH$_3$)$_2$CO and **1b**·(CH$_3$)$_2$CO.

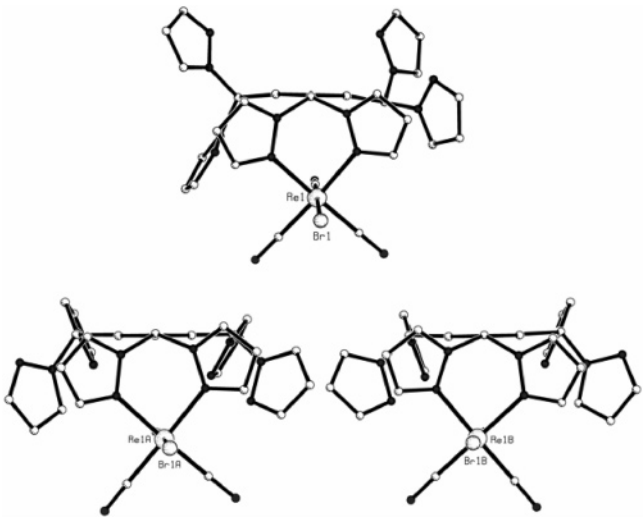

Figure 3. Comparison of the relative conformations of **1** (top) and **1**·(CH$_3$)$_2$CO (bottom) as viewed in the plane of the connecting arene rings. The two crystallographically independent molecules of **1**·(CH$_3$)$_2$CO are shown. Hydrogen atoms are omitted.

among our linked complexes in the related bitopic monometallic compound {*m*-[CH(pz)$_2$]$_2$C$_6$H$_4$}Re(CO)$_3$Br,[10] which displays an analogous conformation in which all four pyrazolyl rings are on the same side of the central ring. In the absence of other sterically demanding, coordinated metal−ligand systems, this surprising conformation with all pyrazolyl rings on the same side of the linking arene group appears to be stable. A driving force for the arrangement may be noncovalent interactions involving the exposed face of the central ring, as discussed below. Even in the unsolvated crystal, the presence of two of the free pyrazolyl rings on the same side as the coordinated site suggests minimal steric conflict among the noncoordinated bis(pyrazolyl)methane sites.

As observed in earlier studies of phenylene-linked bis(pyrazolyl)methane systems,[10] the [Re(CO)$_3$Br] unit of both **1** and **1**·(CH$_3$)$_2$CO is coordinated such that the attached bromine atom is *cis* to the methine hydrogen atom in the boat conformation of the six-membered metallocycle formed by coordination to rhenium. This stereoisomer is the only one formed for **1**, as indicated by ^{1}H NMR and infrared spectra of the bulk sample produced in the reaction. We have previously offered an explanation for this isomeric purity based on transition state theory involving a hydrogen−bromine interaction as well as π bonding between the carbonyl ligands and the central arene ring.[10,23] It is reasonable to assume that such a mechanism is at work in the formation of **1** as well. Also consistent with the earlier dirhenium complexes is the fact that the [Re(CO)$_3$Br] unit is oriented in space such that a carbonyl ligand is positioned over the central arene ring and is participating in intramolecular $\pi_{CO}\cdots\pi_{Ar}$ interactions. Details of these interactions, observed for all the complexes in this work, are presented in Table 4. Both the centroid···centroid distances and the centroid···ring-plane perpendicular distances are given. As expected, each centroid···centroid distance is longer than the corresponding perpendicular distance from the arene ring plane to the centroid of the carbonyl group because none of the carbonyl groups lie directly over the center of the arene ring. The perpendicular distance for each carbonyl group is within accepted values for $\pi\cdots\pi$ interactions.[24]

The supramolecular structure of unsolvated **1** is dominated by multiple hydrogen bonds and one strong $\pi_{pz}\cdots\pi_{pz}$ stacking interaction that combined arrange the molecules into one-dimensional chains of dimers along the *b* direction (Figure 4). No significant noncovalent forces exist between these chains. The repeating unit of these chains can be viewed as dimers formed by two molecules participating in reciprocal 2.96 Å CH···π_{Ar} bonds between a 5-pyrazolyl hydrogen atom of a ligated site on one molecule and the central arene ring of the

(23) Reger, D. L.; Gardinier, J. R.; Pellechia, P. J.; Smith, M. D.; Brown, K. J. *Inorg. Chem.* **2003**, *42*, 7635.
(24) Janiak, C. *J. Chem. Soc., Dalton Trans.* **2000**, 3885.

Table 4. Distances for Intramolecular $\pi_{CO}\cdots\pi_{Ar}$ (Å) Interactions in Rhenium Complexes

compound	carbonyl group	perpendicular distance (ring plane···CO centroid)	ring centroid···CO centroid distance
1	C(73)O(73)	2.970(3)	2.978(3)
1·$(CH_3)_2CO$	C(73A)O(73A)	3.182(3)	3.221(3)
	C(73B)O(73B)	3.250(3)	3.278(3)
2·$(CH_3)_2CO$	C(73)O(73)	3.017(6)	3.043(6)
	C(76)O(76)	3.007(6)	3.046(6)
3·$7CH_3CN$	C(73)O(73)	3.283(5)	3.320(5)
	C(76)O(76)	2.717(6)	3.980(6)
	C(79)O(79)	3.122(5)	3.187(5)
3·$3(CH_3)_2CO$	C(73)O(73)	3.083(6)	3.269(6)
	C(76)O(76)	3.060(6)	3.123(6)
	C(79)O(79)	2.795(9)	4.127(9)
3·$4.5(CH_3)_2CO$	C(73)O(73)	3.010(8)	3.652(8)
	C(76)O(76)	3.045(7)	3.389(7)
	C(79)O(79)	3.489(8)	4.089(8)

other molecule (Figure 4, blue dashed lines). Each dimer is connected to the two adjacent dimers along the *b*-axis through a pair of $\pi_{pz}\cdots\pi_{pz}$ interactions between uncoordinated pyrazolyl groups (Figure 4, red dashed lines). This interaction is fairly strong judging from its relatively short perpendicular (3.59 Å) and centroid···centroid (3.69 Å) distances. Alternatively, the dimers created by this $\pi_{pz}\cdots\pi_{pz}$ interaction can be taken as the base units linked by the CH···π_{Ar} interactions. Combining these two views results in an interlocking arrangement of molecules. Further hydrogen bonding re-enforces this overall supramolecular structure. For instance, two CH···N interactions, at 2.51 and 2.59 Å, exist between molecules reciprocally bound through the $\pi_{pz}\cdots\pi_{pz}$ interaction. The hydrogen donors in these interactions are from a 5-pyrazolyl position on a ligated site and from the central arene ring, respectively. A third CH···N hydrogen bond, involving a methine hydrogen atom at 2.61 Å, re-enforces the CH···π_{Ar} interaction that creates the original dimeric units.

The supramolecular structure of solvated **1**·$(CH_3)_2CO$ consists of sheets of complex molecules in the *ab*-plane that alternate with parallel layers of acetone molecules stacked along the *c*-axis, as shown in Figure 5. Bridging the complex and solvent layers is a network of hydrogen bonds created by two distinct CH···Br interactions (2.84 and 2.93 Å), with acetone molecules as hydrogen donors and bromine atoms from the metal complexes as acceptors. These CH···Br hydrogen bonds work in concert with three types of CH···O interactions (2.53, 2.57, and 2.44 Å), in which the hydrogen donors are the pyrazolyl rings of the complex molecules and the acceptors are the acetone molecules.

No noncovalent interactions exist between molecules in the solvent layer. As a result, the layers of solvent molecules must be held together by the layers of metal complexes, which are supported by a variety of intermolecular interactions. Figure 6 shows a view of the metal complex molecules in the *ab*-plane of **1**·$(CH_3)_2CO$. The two crystallographically distinct molecules, types A and B, each form separate parallel chains running along the *b* direction and alternating with each other along the *a* direction. The molecules of type B are linked together by CH···π_{pz} interactions (2.94 Å; Figure 6, red dashed line), thus forming chains, but no such interactions exist within type A

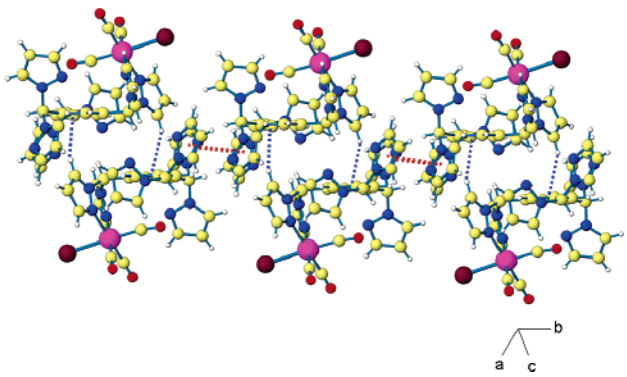

Figure 4. View of the chain of dimeric units along the *b*-axis in unsolvated **1**. CH···π_{Ar} interactions are shown as blue dashed lines and $\pi_{pz}\cdots\pi_{pz}$ interactions as red dashed lines.

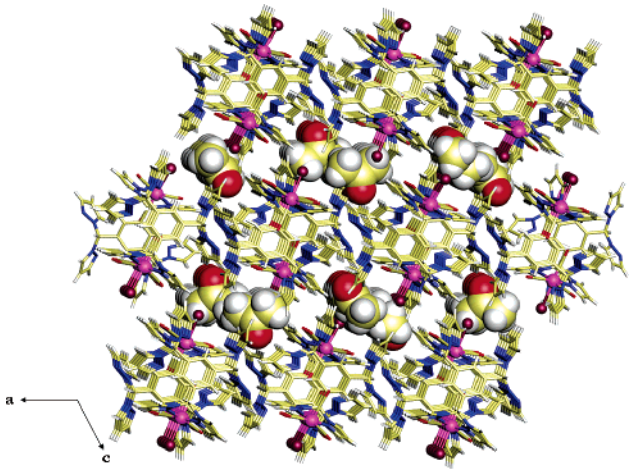

Figure 5. View of the layered structure of **1**·$(CH_3)_2CO$ down the *b*-axis. Acetone molecules are drawn as space-filling models.

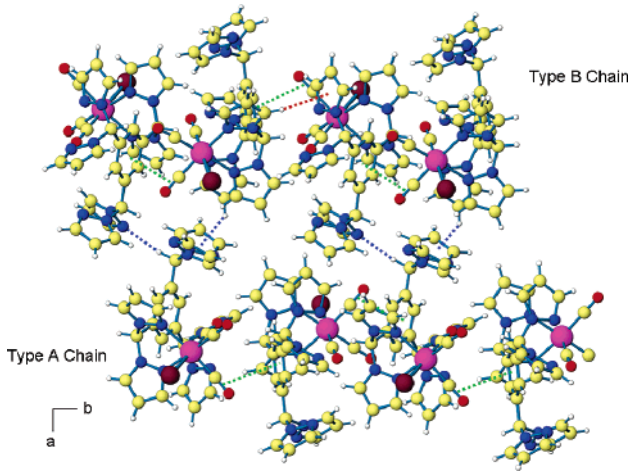

Figure 6. Section of a two-dimensional sheet in the *ab*-plane of **1**·$(CH_3)_2CO$. A CH···π_{pz} interaction between type B molecules is shown by a red dashed line. CH···π_{pz} and CH···N interactions between the two chains are shown as blue dashed lines. $\pi_{CO}\cdots\pi_{Ar}$ interactions within each chain are shown as green dashed lines.

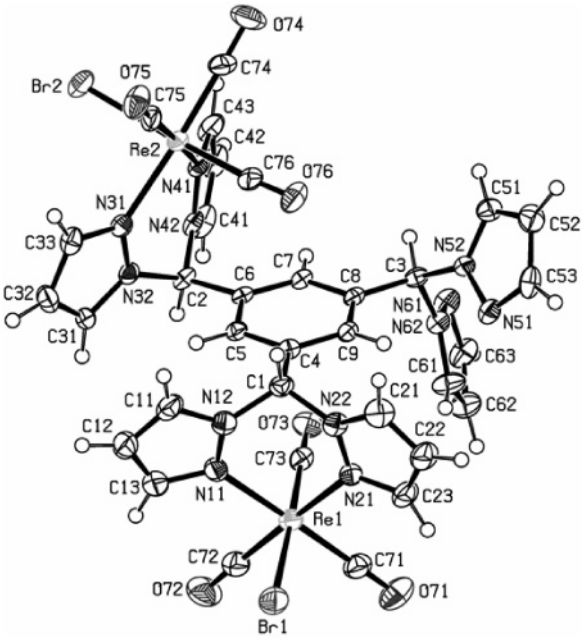

Figure 7. ORTEP drawing of the bimetallic molecule of {μ-1,3,5-[CH(pz)$_2$]$_3$C$_6$H$_3$}[Re(CO)$_5$Br]$_2$·(CH$_3$)$_2$CO (**2**·(CH$_3$)$_2$CO). Ellipsoids are drawn at the 50% probability level.

chains. Instead, the type A chains are assembled through intermolecular 3.64 Å $\pi_{CO}\cdots\pi_{Ar}$ interactions between carbonyl ligands on the rhenium center of one type A molecule and the exposed face of the central arene ring of an adjacent type A molecule. The type B chains are re-enforced by such $\pi_{CO}\cdots\pi_{Ar}$ interactions as well (3.65 Å). In Figure 6, both sets of $\pi_{CO}\cdots\pi_{Ar}$ interactions are shown by green dashed lines. The chains are bound together into sheets by CH$\cdots\pi_{pz}$ interactions between type A molecules in one chain and the type B molecules in an adjacent chain (Figure 6, blue dashed lines). These 2.99 Å interactions are likely weaker than the CH$\cdots$N hydrogen bonds (2.41 Å) that are also binding the chains together. These CH$\cdots$N bonds involve a type A methine hydrogen atom and an uncoordinated type B pyrazolyl nitrogen atom. Additional CH$\cdots$N hydrogen bonds present re-enforce the structure described and are not pictured.

Among the arene-linked bi- and tritopic bis(pyrazolyl)methane complexes we have studied, **1**·(CH$_3$)$_2$CO presents the first example of *inter*molecular $\pi_{CO}\cdots\pi_{Ar}$ interactions. This feature is largely due to the fact that in the majority of the complexes the arene ring is partially blocked by a coordinated metal−ligand system and therefore lacks intermolecular access to adjacent molecules. The only other complex investigated in which an exposed arene ring face is present in the crystal structure is {*m*-[CH(pz)$_2$]$_2$C$_6$H$_4$}Re(CO)$_3$Br, but no intermolecular $\pi_{CO}\cdots\pi_{Ar}$ interactions are observed for this compound.

The dirhenium complex **2** crystallizes from acetone−diethyl ether in a single form as the solvate {μ-1,3,5-[CH(pz)$_2$]$_3$C$_6$H$_3$}-[Re(CO)$_5$Br]$_2$·(CH$_3$)$_2$CO (**2**·(CH$_3$)$_2$CO; space group *P*1). Figure 7 shows an ORTEP representation of the metal complex, and selected bond distances and angles are given in Table 5. As observed in previously studied dirhenium complexes of arene-linked ligands,[10] the [Re(CO)$_3$Br] units in **2**·(CH$_3$)$_2$CO are positioned on opposite sides of the central arene ring. As in both of the structures of **1**, each [Re(CO)$_3$Br] unit is oriented such that a carbonyl ligand is participating in intramolecular $\pi_{CO}\cdots\pi_{Ar}$ interactions with the central ring (see Table 4 for details), and the only stereoisomer produced was the one in

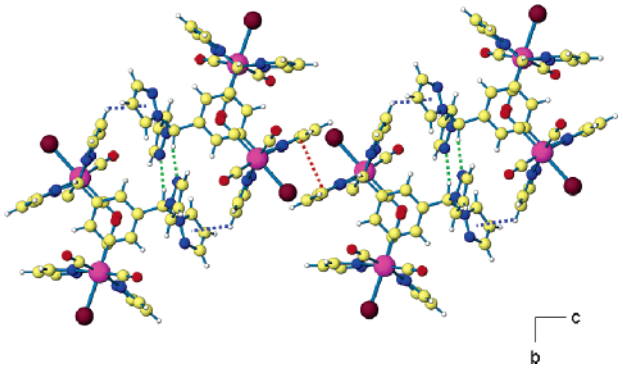

Figure 8. Section of a chain of complex molecules in **2**·(CH$_3$)$_2$-CO as viewed down the *a*-axis. Noncovalent interactions are shown by red ($\pi_{pz}\cdots\pi_{pz}$), blue (CH$\cdots\pi_{pz}$), and green (CH$\cdots$N) dashed lines.

Table 5. Selected Bond Distances (Å) and Angles (deg) for 2·(CH$_3$)$_2$CO

Re(1)−N(11)	2.184(6)
Re(1)−N(21)	2.180(6)
Re(1)−C(71)	1.919(8)
Re(1)−C(72)	1.902(8)
Re(1)−C(73)	1.917(7)
Re(1)−Br(1)	2.6313(8)
Re(2)−N(31)	2.183(6)
Re(2)−N(41)	2.185(6)
Re(2)−C(74)	1.895(8)
Re(2)−C(75)	1.908(7)
Re(2)−C(76)	1.922(7)
Re(2)−Br(2)	2.6202(8)
N(11)−Re(1)−N(21)	84.4(2)
N(11)−Re(1)−Br(1)	83.09(15)
N(21)−Re(1)−Br(1)	82.95(15)
C(71)−Re(1)−Br(1)	94.6(2)
C(71)−Re(1)−N(11)	177.6(3)
C(71)−Re(1)−C(72)	87.0(3)
N(31)−Re(2)−N(41)	82.6(2)
N(31)−Re(2)−Br(2)	86.29(14)
N(41)−Re(2)−Br(2)	84.47(14)
C(74)−Re(2)−Br(2)	89.9(2)
C(74)−Re(2)−N(31)	176.1(3)
C(74)−Re(2)−C(75)	86.2(3)

which the bromine atom is *cis* to the methine hydrogen atom in the metallocycle formed upon coordination to rhenium.

Noncovalent interactions in **2**·(CH$_3$)$_2$CO organize the metal complex molecules into one-dimensional chains parallel to the *c*-axis (Figure 8), and these chains are further and weakly joined into two-dimensional sheets in the *ac*-plane. A strong $\pi_{pz}\cdots\pi_{pz}$ interaction, shown by the red dashed lines in Figure 8, exists between coordinated pyrazolyl rings that are nearly perfectly parallel (dihedral angle between planes = 0.02°; centroid$\cdots$centroid distance = 3.75 Å; shortest perpendicular distance = 3.37 Å). Supporting these $\pi_{pz}\cdots\pi_{pz}$ interactions are reciprocal CH$\cdots$Br hydrogen bonds (not pictured) between Br(2) and the 5-pz hydrogen atom on the nearby pyrazolyl ring of an adjacent molecule. The hydrogen donors are associated with the same ligating groups undergoing the $\pi_{pz}\cdots\pi_{pz}$ stack. The dimers formed by the two noncovalent associations just described are further linked with adjacent dimers by a combination of CH$\cdots\pi_{pz}$ and CH$\cdots$N hydrogen bonds. The blue dashed lines of Figure 8 outline the CH$\cdots\pi_{pz}$ interactions between a 4-pz hydrogen donor of a coordinated group with an uncoordinated pyrazolyl ring acceptor (CH$\cdots$centroid distance and angle are 2.76 Å and 123°). In support of this interaction is the 2.33 Å CH$\cdots$N hydrogen bond at a 169° angle (green dashed lines) between H(3), the methine hydrogen atom from an uncoordinated ligating group, and a nitrogen atom from the uncoordinated

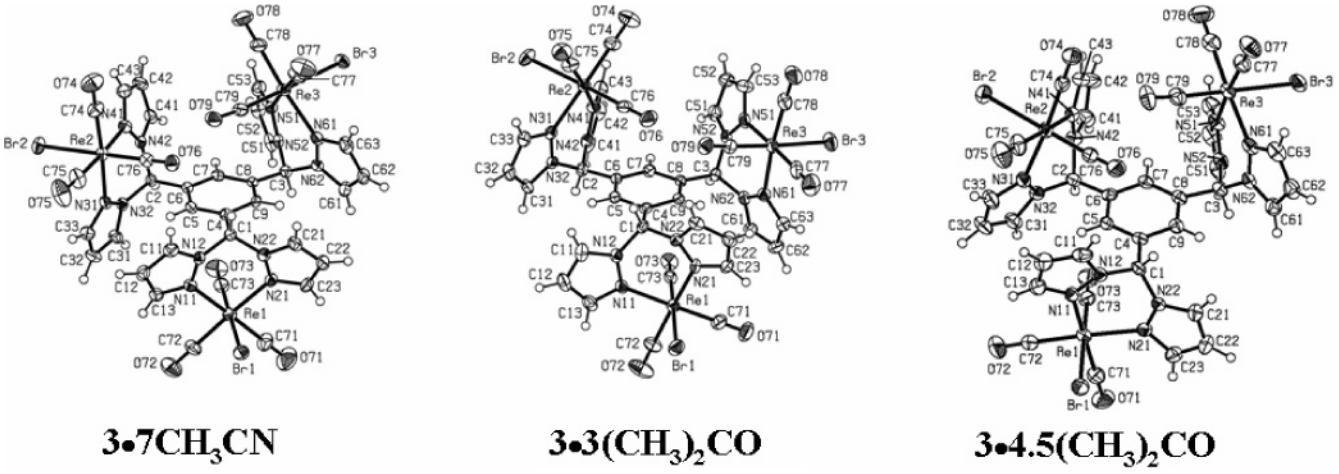

Figure 9. ORTEP drawings of the trimetallic molecules of $\{\mu$-1,3,5-$C_6H_3[CH(pz)_2]_3\}[Re(CO)_3Br]_3\cdot 7CH_3CN$ (**3**·$7CH_3CN$), $\{\mu$-1,3,5-$C_6H_3[CH(pz)_2]_3\}[Re(CO)_3Br]_3\cdot 3(CH_3)_2CO$ (**3**·$3(CH_3)_2CO$), and $\{\mu$-1,3,5-$C_6H_3[CH(pz)_2]_3\}[Re(CO)_3Br]_3\cdot 4.5(CH_3)_2CO$ (**3**·$4.5(CH_3)_2CO$). Ellipsoids are drawn at the 50% probability level.

ligating group of an adjacent molecule. Both of these interactions are reciprocal. The two-dimensional supramolecular structure of **2**·$(CH_3)_2CO$ is completed by weak CH···O hydrogen bonds (not pictured) between a 5-pz hydrogen atom on a free pyrazolyl group and an oxygen atom from a carbonyl ligand on an adjacent chain along the *a*-axis, thereby forming sheets in the *ac*-plane. The acetone molecules in **2**·$(CH_3)_2CO$ are positioned in small cavities between the sheets of metal complex molecules and participate in little to no hydrogen-bonding interactions with other solvent molecules or with metal complex molecules.

The recrystallization of $\{\mu$-1,3,5-$C_6H_3[CH(pz)_2]_3\}[Re(CO)_3Br]_3$ (**3**) by the vapor diffusion of diethyl ether into separate acetonitrile and acetone solutions yielded three distinct species. From the acetonitrile solution crystallized a compound in the chiral orthorhombic space group $P2_12_12_1$ with seven *ordered* acetonitrile molecules of solvation, $\{\mu$-1,3,5-$C_6H_3[CH(pz)_2]_3\}$-$[Re(CO)_3Br]_3\cdot 7CH_3CN$ (**3**·$7CH_3CN$). From the same acetone solution crystallized two pseudopolymorphs, one in the monoclinic space group $P2_1/c$ with three acetone molecules of solvation, $\{\mu$-1,3,5-$C_6H_3[CH(pz)_2]_3\}[Re(CO)_3Br]_3\cdot 3(CH_3)_2CO$ (**3**·$3(CH_3)_2$-CO), and the other in the triclinic space group $P\bar{1}$ with 4.5 acetone molecules of solvation per asymmetric unit, $\{\mu$-1,3,5-$C_6H_3[CH(pz)_2]_3\}[Re(CO)_3Br]_3\cdot 4.5(CH_3)_2CO$ (**3**·$4.5(CH_3)_2CO$).

Figure 9 shows ORTEP representations of the trimetallic molecules of all three crystalline species. Selected bond distances and angles are compared in Table 6. The trimetallic molecules in each crystalline species differ from one another in the relative orientations of the $-CH(pz)_2[Re(CO)_3Br]$ units about the central arene ring, particularly the positions of the carbonyl groups (see Table 4). These differences are possible through the rotational freedom of the bis(pyrazolyl)methane groups about the arene ring and may be caused by varying degrees of noncovalent interactions in the supramolecular structures (see below). In each structure, the "two up−one down" conformation, invoked in interpreting the NMR data above, is observed. Spectral data indicate that the amorphous solid **3** is formed exclusively as one stereoisomer. The structures of all three crystalline forms show that this isomer is the one in which each bromine atom bound to rhenium is *cis* to its respective methine hydrogen atom and that a carbonyl ligand bound to rhenium participates in intramolecular $\pi_{CO}\cdots\pi_{Ar}$ interactions (Table 4). The $[Re(CO)_3Br]$ units in **3**, therefore, have the same relative orientations as those in **1** and **2**.

The crystalline metal complex **3**·$7CH_3CN$ consists of a layered structure analogous to the one discussed above for **1**·$(CH_3)_2CO$. In **3**·$7CH_3CN$, layers of metal complex molecules alternate with layers of acetonitrile molecules in stacking along the *c*-axis (Figure 10). Multiple hydrogen bonds bridge the solvent and complex molecule layers. In the complexes, the hydrogen donors include the methine groups of the bis(pyrazolyl)methane units and the 3- and 5-positions of the pyrazolyl rings. The acceptors associated with these donors are the acetonitrile molecules. The methyl groups of the solvent molecules also act as donors to the rhenium-bound bromine atoms and the oxygen atoms of the carbonyl ligands in the

Table 6. Selected Bond Distances (Å) and Angles (deg) for 3·7CH₃CN, 3·3(CH₃)₂CO, and 3·4.5(CH₃)₂CO

	3·$7CH_3CN$	**3**·$3(CH_3)_2CO$	**3**·$4.5(CH_3)_2CO$
Re(1)−N(11)	2.177(4)	2.190(5)	2.184(6)
Re(1)−N(21)	2.177(4)	2.175(5)	2.172(6)
Re(1)−C(71)	1.910(5)	1.920(7)	1.927(7)
Re(1)−C(72)	1.919(5)	1.910(6)	1.918(8)
Re(1)−C(73)	1.903(5)	1.902(8)	1.912(7)
Re(1)−Br(1)	2.6386(6)	2.6355(8)	2.6293(8)
Re(2)−N(31)	2.184(4)	2.179(5)	2.176(5)
Re(2)−N(41)	2.169(4)	2.183(5)	2.172(6)
Re(2)−C(74)	1.917(5)	1.916(7)	1.906(7)
Re(2)−C(75)	1.911(5)	1.919(7)	1.913(8)
Re(2)−C(76)	1.910(5)	1.904(7)	1.911(7)
Re(2)−Br(2)	2.6245(6)	2.6247(7)	2.6280(8)
Re(3)−N(51)	2.175(4)	2.184(6)	2.167(6)
Re(3)−N(61)	2.168(4)	2.177(5)	2.173(6)
Re(3)−C(77)	1.918(5)	1.921(8)	1.902(7)
Re(3)−C(78)	1.904(5)	1.911(7)	1.920(9)
Re(3)−C(79)	1.905(5)	1.901(7)	1.898(8)
Re(3)−Br(3)	2.6395(5)	2.6242(7)	2.6307(8)
N(11)−Re(1)−N(21)	86.83(15)	83.86(19)	85.2(2)
N(11)−Re(1)−Br(1)	83.96(10)	87.35(14)	83.23(14)
N(21)−Re(1)−Br(1)	81.81(10)	83.72(14)	84.45(15)
C(71)−Re(1)−Br(1)	90.97(18)	91.7(2)	91.2(2)
C(71)−Re(1)−N(11)	174.9(2)	177.8(3)	174.2(3)
C(71)−Re(1)−C(72)	88.7(2)	87.2(3)	88.4(3)
N(31)−Re(2)−N(41)	84.50(14)	84.46(19)	84.1(2)
N(31)−Re(2)−Br(2)	83.55(10)	85.14(14)	84.74(15)
N(41)−Re(2)−Br(2)	86.47(11)	84.06(14)	85.08(15)
C(74)−Re(2)−Br(2)	90.96(17)	92.8(2)	90.2(2)
C(74)−Re(2)−N(31)	173.99(19)	176.7(3)	174.7(3)
C(74)−Re(2)−C(75)	88.6(2)	88.6(3)	89.5(3)
N(51)−Re(3)−N(61)	85.03(14)	84.2(2)	84.7(2)
N(51)−Re(3)−Br(3)	84.15(11)	86.33(13)	83.89(15)
N(61)−Re(3)−Br(3)	83.47(10)	82.61(13)	83.89(15)
C(77)−Re(3)−Br(3)	94.45(16)	92.9(2)	91.4(2)
C(77)−Re(3)−N(51)	177.0(2)	177.2(2)	175.2(3)
C(77)−Re(3)−C(78)	89.8(2)	88.0(3)	88.8(3)

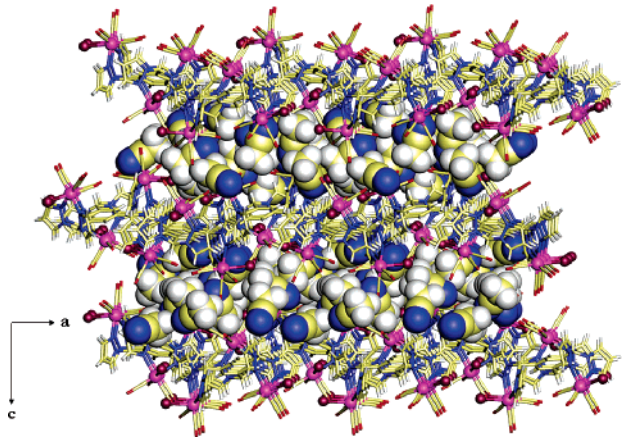

Figure 10. Layered structure of **3**·7CH_3CN as viewed down the *b*-axis. Acetonitrile molecules are shown as space-filling models.

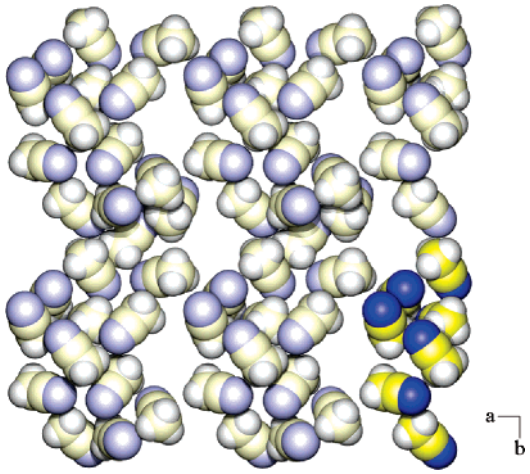

Figure 11. View in the *ab*-plane of a sheet of ordered acetonitrile molecules in **3**·7CH_3CN. The repeating unit of seven molecules is highlighted in the lower right corner of the sheet.

complexes. There is also a long (3.33 Å) CH···π_{pz} involving an acetonitrile hydrogen donor. The supramolecular structure of **3**·7CH_3CN is particularly unusual in the large number (seven) of ordered acetonitrile molecules present. The sheet of acetonitrile molecules shown in Figure 11 lies in the *ab*-plane and extends in both the *a* and *b* directions. A unique set of seven solvent molecules is highlighted. There is little to no hydrogen bonding between molecules in this layer.

Because of the lack of extensive intermolecular interactions in the acetonitrile layer, the layers of metal complex molecules largely organize these solvent layers. The supramolecular structure of the metal complex layers in **3**·7CH_3CN is dominated by a set of cooperative noncovalent interactions that we have previously termed the "quadruple pyrazolyl embrace".[5b] In the pyrazolyl embrace, four pyrazolyl rings from two nearby bis(pyrazolyl)methane sites are associated through concerted CH···π_{pz} and π_{pz}···π_{pz} interactions, forming an organized supramolecular motif. The pyrazolyl embrace has been found to be a common feature in poly(pyrazolyl)borate and -methane compounds. As shown in Figure 12, the complex molecules of **3**·7CH_3CN are linked by the pyrazolyl embrace into chains propagating along the *a* direction while winding in the *ab*-plane. The propagation of these chains imparts the homochiral feature of the crystals. There are no important interactions between adjacent chains. The CH···π_{pz} interactions of the embrace are atypical, with one involving a 5-pz hydrogen atom (H42) rather than the most commonly observed 4-pz hydrogen atom. Also,

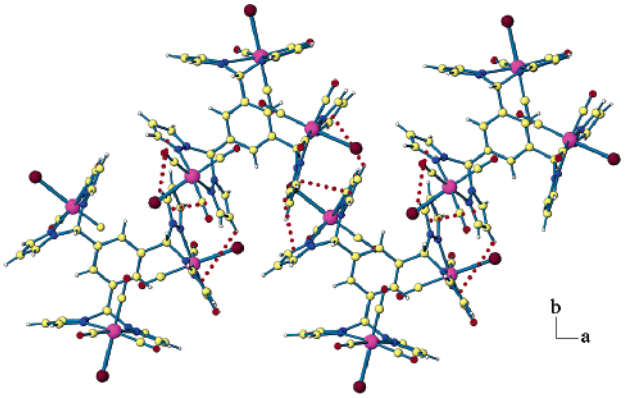

Figure 12. Alternating chain formed by the quadruple pyrazolyl embrace (red dashed lines) in **3**·7CH_3CN.

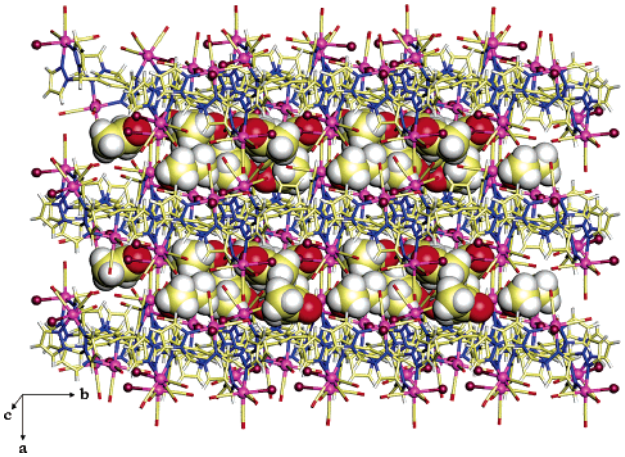

Figure 13. Layered structure of **3**·3$(CH_3)_2CO$ as viewed down the *c*-axis. Acetone molecules are shown as space-filling models.

the CH···centroid distances, 3.38 and 3.33 Å, are at the upper limit of typical values for these interactions.[5b]

The overall supramolecular motif of the acetone-solvated pseudopolymorph **3**·3$(CH_3)_2CO$ is similar to the structures of **1**·$(CH_3)_2CO$ and **3**·7CH_3CN in that **3**·3$(CH_3)_2CO$ exhibits a sandwich structure resulting from the alternate stacking of sheets of complex molecules with layers of solvent molecules along the *a*-axis (Figure 13). As in the other two layered structures, hydrogen bonds in **3**·3$(CH_3)_2CO$ bridge the metal complex and solvent layers. The hydrogen donors in **3**·3$(CH_3)_2CO$ are methine groups and a 5-pyrazolyl position, and the oxygen atoms of acetone serve as acceptors. There are no intermolecular interactions within the acetone layers. The metal complex layers, therefore, provide part of the cohesion for the solvent layers, as was observed for the previous two layered structures. The layers of metal complex molecules in **3**·3$(CH_3)_2CO$ are not composed of independent chains as in **3**·7CH_3CN but rather two-dimensional networks organized by pyrazolyl embrace interactions (Figure 14). Thus, each bis(pyrazolyl)methane ligating site is participating in noncovalent interactions with an appropriate site from an adjacent molecule.

The second structure from acetone, **3**·4.5$(CH_3)_2CO$, displays no extended structure among complex molecules beyond the dimeric unit shown in Figure 15, and no layered structure is observed. Solvent molecules are intercalated between trimetallic molecules, and noncovalent interactions among complex molecules are notably weaker compared with the previous two compounds, as evidenced by longer distances for the observed CH···π_{pz} and π_{pz}···π_{pz} interactions. For instance, CH···π_{pz} interactions for the pyrazolyl embrace (Figure 15, red dashed

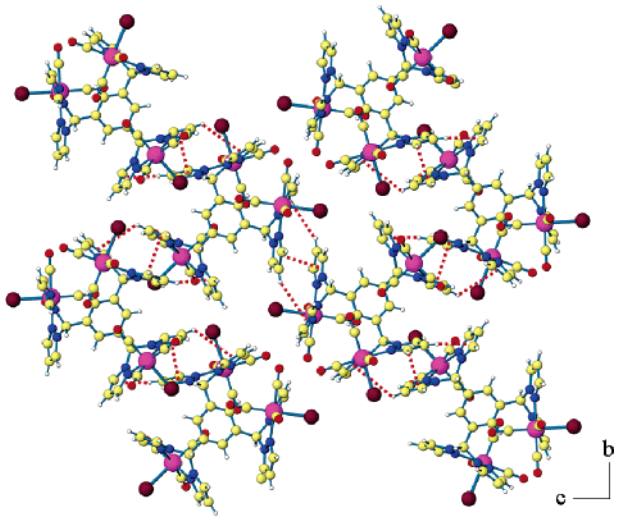

Figure 14. View of the *bc*-plane in **3**·3$(CH_3)_2$CO organized by quadruple pyrazolyl embrace interactions (red dashed lines).

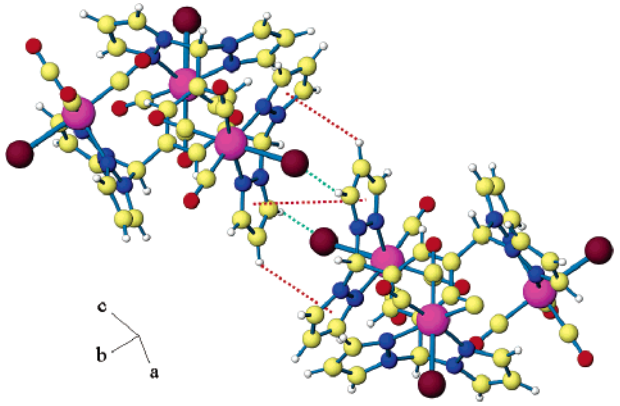

Figure 15. Dimeric association of complex molecules in **3**·4.5$(CH_3)_2$CO organized by quadruple pyrazolyl embrace interactions (red dashed lines) and CH···Br interaction (green dashed lines).

lines) in the structure of **3**·4.5$(CH_3)_2$CO are at 3.34 Å and $\pi_{pz}\cdots\pi_{pz}$ stacking occurs at a distance of 4.10 Å. Average values for these interactions are 2.71 and 3.71 Å, respectively.[5b] The elongation of these distances appears to be caused by a distortion of the pyrazolyl embrace that allows a CH···Br interaction with a distance of 2.81 Å (Figure 15, green dashed lines). An analogous distortion is noticeable in the structure of **2**·$(CH_3)_2$CO described above, where CH···Br bonds also seem to have disrupted the pyrazolyl embrace to such an extent that the interaction cannot be confidently said to exist in that structure.

During our studies of the bitopic ligands *m*-[CH$(pz)_2]_2C_6H_4$, *p*-[CH$(pz)_2]_2C_6H_4$, and *p*-[CH$(^{4Bn}pz)_2]_2C_6H_4$ (^{4Bn}pz = 4-benzyl-1-pyrazolyl), all of the bimetallic [$Re(CO)_3Br$] species adopted a conformation in which the two ligating sites were on opposite sides of the ring.[10] The compound reported here, {μ-1,3,5-[CH$(pz)_2]_3C_6H_3$}[$Re(CO)_5Br]_3$ (**3**), is therefore the first complex we have observed in these rigidly linked systems with two metal centers on the same side of the central arene ring. The steric strain of having two octahedral tricarbonylrhenium centers in such proximity is relieved in this system by rotation of the bis(pyrazolyl)methane groups about the central ring, thus decreasing the π-orbital overlap between the central ring and a carbonyl group bound to rhenium. The presence of two metallic units on the same side of the ring prevents either of these proximate carbonyl ligands in each molecule from being directly over the center of the ring (see Table 4), a conformation observed in the previous study with bimetallic complexes,[10] but the extent to which the carbonyl ligands have "slipped" off the central ring may be influenced more by crystal packing (including noncovalent interactions, vide supra) and electronic effects than by steric constraints.

Each of the complexes in this study displays *intra*molecular CH···π_{pz} interactions in the solid state between an arene hydrogen atom and an adjacent pyrazolyl ring. The distances for these interactions are in the range of 2.6 to 2.9 Å, and each interaction always involves at least one coordinated pyrazolyl ring. The presence of interactions in the crystalline forms supports the interpretation of the NMR data presented earlier, in which for the complexes, arene proton signals adjacent to at least one coordinated pyrazolyl ring are shifted upfield relative to those in the free ligand.

Conclusions

Synthetic methods for the selective preparation and purification of the mono-, di-, and trirhenium complexes {1,3,5-[CH$(pz)_2]_3C_6H_3$}$Re(CO)_3Br$ (**1**), {μ-1,3,5-[CH$(pz)_2]_3C_6H_3$}[$Re(CO)_5Br]_2$ (**2**), and {μ-1,3,5-[CH$(pz)_2]_3C_6H_3$}[$Re(CO)_5Br]_3$ (**3**) from the reactions of $Re(CO)_5Br$ and the tritopic, third-generation bis(pyrazolyl)methane ligand 1,3,5-[CH$(pz)_2]_3C_6H_3$ (**L**) have been developed. The use of stoichiometric amounts of starting reagents, whether attempting to prepare the mono-, bi-, or trimetallic complex, always resulted in the isolation of a mixture of all three compounds. This problem was obviated in making the monorhenium complex by using a large excess of the ligand such that **1** was produced exclusively. This solution, however, was not available for the bimetallic species, and the crude product **2** had to be recrystallized to separate it from the other species. In contrast to the preparation of the monometallic compound, the trimetallic species could not be obtained free of the aforementioned contaminants regardless of the size of the excess of $Re(CO)_5Br$ used, and extraction of the impurities was necessary. The starburst ligand **L** is the second of the rigid, arene-linked bis(pyrazolyl)methane ligands we have studied that has proven useful for the preparation of metal complexes with at least one open ligating site. Because a major goal of these studies is to provide a convenient route to heterometallic complexes of homomultitopic ligands, synthetic studies of the potential of **1** and **2** to serve as intermediates to such complexes are currently underway.

All of the tricarbonylrhenium(I) complexes we have prepared with rigid, arene-linked ligands have shown themselves predisposed to specific intramolecular and supramolecular features in the crystalline form. Each complex contains intramolecular CH···π_{pz} interactions between the central arene ring hydrogen atoms and coordinated pyrazolyl rings (as well as uncoordinated rings in some examples). Additionally, each complex exhibits intramolecular $\pi_{CO}\cdots\pi_{Ar}$ interactions and, in one instance, intermolecular $\pi_{CO}\cdots\pi_{Ar}$ when the crystalline conformation of the complex allows intermolecular access to the central π region. The quadruple pyrazolyl embrace[5b] becomes an important organizing factor for the trimetallic complexes, but is not dominant in the other compounds.

Of the five solvated crystal structures reported above, three exhibit the structural motif of alternating layers of complex and solvent molecules. Thus, **1**·$(CH_3)_2$CO, **3**·7CH_3CN, and **3**·3$(CH_3)_2$CO contain two-dimensional sheets of complex molecules, which are themselves held together through various noncovalent interactions, that stack upon acetone or acetonitrile layers through noncovalent attractions (typically hydrogen bonds). In all three structures, there are no intrasheet interactions in the

solvent layers; they are entirely organized by their interactions with the sheets of complex molecules. This separation of complex and solvent molecules is indicative of the stability of the supramolecular assemblies of the complex molecules as brought about by the potential for noncovalent interactions intentionally designed into the ligands. Consistent supramolecular properties such as the ones described above may be useful in understanding and designing metal−ligand systems with predictable intermolecular interactions.

Acknowledgment. We thank Radu Semeniuc for helpful discussion and the National Science Foundation (CHE-0414239) for financial support. We also thank the Alfred P. Sloan Foundation for support of R.P.W. The Bruker CCD single crystal diffractometer was purchased using funds provided by the NSF Instrumentation for Materials Research Program through Grant DMR:9975623.

Supporting Information Available: X-ray crystallographic files in CIF format for all structures reported. An Arrhenius plot and free energy calculations in text format. This information is available free of charge via the Internet at http://pubs.acs.org.

OM0508684